

Analytical Modeling of Insulated Dipole Applicators for Interstitial Hyperthermia: a Review

Florence SAGNARD

Institute of Electronics and Telecommunication of Rennes, INSA, 20 av. des Buttes de Coësmes, 35043 Rennes, France
University of Marne-La-Vallée, Cité Descartes, Champs-sur-Marne, 77454 Marne-La-Vallée Cedex, France

sagnard@univ-mlv.fr, florence.sagnard@equipement.gouv.fr

Abstract. *Microwave hyperthermia appears as an adjuvant technique to heat relatively small tumors in a minimally invasive way. As this technique is based on interstitial antennas, we propose a review of the physical phenomena involved in the radiation of such antennas in a dispersive medium, using the different analytical modeling developed since the 1970's. These modeling have been implemented in a freely available software tool, that will allow antenna designers and medical researchers to perform rapid parameter studies to further understand the role of the several parameters involved; this tool will also help the interpretation of results issued from numerical simulations. Simulation results associated with different antenna geometries are presented and compared to results obtained by several authors.*

Keywords

Insulated antenna, dipole antennas, radiation, hyperthermia, dissipative media, microwave antenna arrays.

1. Introduction

Hyperthermia has emerged as a promising alternative or adjunct to other forms of cancer therapy. It uses either electromagnetic field, ultrasound or perfusion based methods to raise the tumor temperature above 40°C while maintaining the surrounding normal tissue below this temperature. All the techniques used can be distinguished by the spatial scale at which thermal ablation is induced: local hyperthermia, regional hyperthermia, and whole-body hyperthermia.

Among more or less invasive electromagnetic techniques, two types can be considered depending on the range of frequency used [1-6]: at first, capacitive and inductive coupled radiofrequency (RFA, RadioFrequency Ablation) methods (300 kHz-1 MHz) are based on resistive currents, because the displacement currents appear negligible at these frequencies. Secondly, microwave radiative applicators (300 MHz-2.45 GHz), based on propagative waves generated by one or several antennas, are positioned in contact with the malignant tissue in order to deposit a focused electromagnetic energy in a limited volume (2 to

5 cm) in the near-field zone of the antenna system. In general, the electromagnetic energy absorption at the applied frequency is proportional to the tissue conductivity and to the square root of the dielectric constant of the targeted material; usually such an absorption leads to local temperature elevation of cells belonging to malignant tissues between approximately 40°C and 45°C for 30 to 60 minutes. So, an efficient coupling of the electromagnetic energy to the malignant tissue is necessary to ensure a sufficient transfer of energy inside the tumor, and a heating distribution as uniform as possible with minimal unwanted hot spots. Due to its intensive metabolic activity, malignant tissue has a higher conductivity than normal tissue, as well as the dielectric constant at the applied frequencies is also higher in the malignant tissue than in the healthy one [7].

The aim of this paper is to provide a review of analytical modeling of microwave insulated antennas encountered in the literature. In general, the modeling associated with hyperthermia applications is composed of two parts: an electromagnetic modeling and a thermal modeling. The present work concerns a detailed study relative to the electromagnetic part of the initial problem. The electromagnetic models issued from the literature have been implemented in the Matlab interface, and are available on request¹. The insulated dipole applicator, first modeled by R. W. P. King in the 1970's [8-10], was concerning a symmetrical coaxial antenna supposed to be inserted in a highly dissipative medium. Afterwards, the modeling has been numerically improved by J. P. Casey in 1986 [11], and extended by M. F. Iskander in 1989 [12], K. L. Clibbon [13] in 1994, and L. K. Wu in 1996 [14] to further consider a multisection antenna and possibly non symmetrically fed. Such an analytical modeling appears useful to antenna designers and medical researchers to further understand the physical phenomena involved in electromagnetic absorption, to study the influence of the different parameters, and to interpret numerical simulations. Once the SAR (Specific Absorption Rate) distribution is determined, it serves later as a source in the bioheat equation to calculate the temperature distribution in the tissue region.

¹ sagnard@univ-mlv.fr ;
florence.sagnard@equipement.gouv.fr

Moreover, we have studied the distribution of insulated dipole antennas in an array in order to obtain a more uniform heating pattern; the heating pattern is controlled by choosing relative phases between antennas in order to obtain constructive and/or destructive interferences features of the electromagnetic fields radiated by the antennas [15], [16]. Finally, a few simulation results obtained with the Matlab toolbox are presented; these simulations have been analyzed and compared with the results issued from the literature.

2. General Formulation

The modeling of a symmetrical uniform coaxial dipole applicator surrounded by a dissipative medium, as first proposed by R. W. P. King in the 1970's at frequency 915 MHz [8-10], can be visualized in Fig. 1a. The dimension of the dipole is close to the wavelength $\lambda_L=2\pi/\beta_L$ (β_L is the wavenumber), which characterizes the antenna electromagnetic length as it is surrounded by a lossy dielectric medium. Such an antenna produces propagative waves which are rapidly attenuated in the near-field zone of the surrounding medium. This medium acts as an imperfect outer conductor for the antenna; thus, it can be modeled as a coaxial transmission line. A non-lossy insulation medium inserted between the central conductor with a finite conductivity and the outer medium with an infinitely extent allows the generation of electromagnetic waves which propagate inside the outer medium. Moreover, by applying a simple scaling of size and frequency to the antenna geometry, other working frequencies can be considered. It must be underlined that, in such a structure, the current distribution along the inner conductor of the antenna depends closely on the insulation layer, thus leading to a relatively complicated wavenumber current determination as it is quite different from the wavenumber of the outer medium.

As the determination of the distribution of energy absorbed in the outer medium implies the knowledge of the electric field radiated mainly in the near-field zone, a solution was first given by R. W. P. King, using approximate numerical calculations [8]. However, such a solution was inadequate near the surface of the insulated antenna, which led J. P. Casey to provide improvements [11]. Later in 1989, M. F. Iskander proposed an approximate solution for a thin-wire antenna which led to very similar electric field distribution in the outer medium [12]; however, this model cannot evaluate the electric field inside the antenna. Such an approach allows to consider a non uniform coaxial antenna made of several sections to improve the uniformity of the electromagnetic energy absorbed in the near-field region; in such an antenna structure, the sections are characterized by different inner conductor radii and insulation thicknesses as visualized on Fig. 1b. The approximate model is based on the decomposition of the current distribution along the antenna as a linear array of point sources representing infinitesimal electric dipoles assumed to be

distributed along the insulation surface. In such a case, the electric field radiated in the outer medium is the sum of the infinitesimal electric fields produced by all the aligned point-sources.

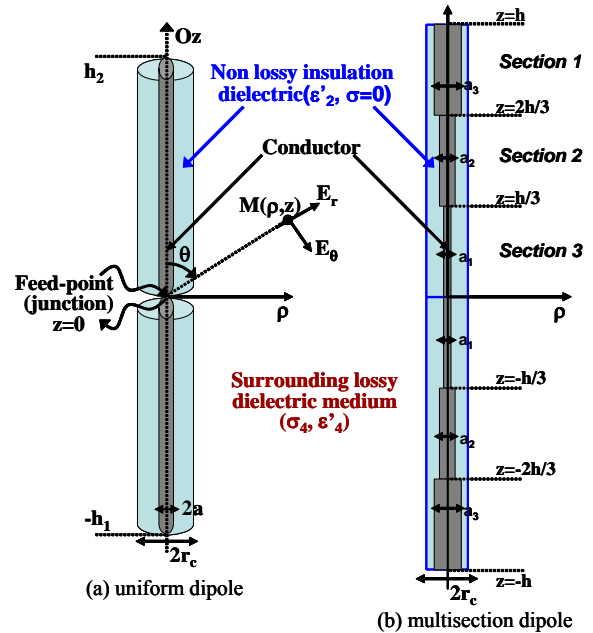


Fig. 1. Geometries of two types of insulated dipoles.

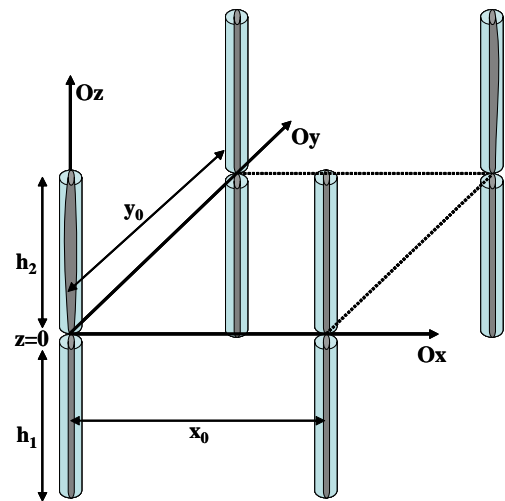


Fig. 2. Square array of 4 identical insulated dipoles in the plane (xOy).

Because the highest electromagnetic absorption generally occurs in the near zone of the feed-point and on the antenna surface, the solution to provide a more uniform absorption around the antenna was to break down the antenna length into several sections characterized by proper conductor and insulation layer thicknesses, thus leading to different radiation efficiencies. Thus, a section with a thinner (thicker) insulation layer will cause higher (lower) energy loss, mainly induced by ohmic losses in the near-field zone of the antenna. The solution is then to position a thinner insulation layer close to the feed-point. Moreover, the association of antennas distributed in an array (Interstitial Microwave Antenna Array Hyperthermia system, IMAAH) with a spacing of about 1-2 cm between the an-

tennas to which a specific driving phase has been applied, is discussed (see Fig. 2) [14-16]; this phase represents an additional parameter that allows to control the heating pattern, and particularly to push away hot spots at the boundary of the tumor to reduce the cooling effect generated by blood flow.

3. Modeling Based on the Transmission Line Approach

3.1 Overview of the Transmission Line Approach

In King's developments [8-10], an insulated dipole antenna of length $2h$ and aligned along axis Oz is driven at its center ($z = 0$) (see Fig. 1a). As it is terminated by two open circuits at both ends, such an antenna can be considered as an open coaxial cable. Thus, it can be analytically modeled using the transmission line theory. The modeling presented in this paper is valid either for dipole or monopole antennas.

Following R. W. P. King's developments, the external conductor (medium 4) is supposed to be made of the surrounding medium represented by an infinite and isotropic lossy dielectric medium. The inner conductor (medium 1) with the radius a is characterized by a high but finite conductivity. To prevent radial currents from flowing into the outer lossy medium, which contribute to decrease the axial current along the antenna, a non-lossy dielectric medium (equivalent effective single-layer medium with index $2e$) with the outer radius r_c is placed between the inner conductor and the surrounding medium; the inner conductor is thus insulated from the surrounding medium. Depending on the applications, the insulation medium can be made of superimposed non-lossy dielectric layers (for example, two layers made of media 2 and 3 [10]). The so-called insulated antenna is characterized by numerous parameters that can be adjusted to change its radiating properties; these parameters include the length h , the ratio r_c/a of the radius of the insulating medium r_c to the radius of the inner conductor a , the constant β_L (β_L is the real part of the wavenumber $k_L = \beta_L + j\alpha_L$ associated with the propagating current inside the inner conductor), and the wavenumber ratios $|k_4/k_{2e}|$ in media 4 and 2.

The analytical modeling initially proposed by R. W. King, and further extended by different authors [11-13], supposes several initial conditions and parameters such as:

- The operating frequency:
200 MHz $< f \leq$ 2.45 GHz.
- The half antenna length h in the case of a dipole, which is generally defined in order to obtain a resonant structure with $\beta_L h = \pi/4$ or $\pi/2$.
- The cross-section of the antenna is electrically small (higher propagation modes become negligible, end-

effects are small, and the antenna current is only axial), and the wavenumber of the outer medium is large compared to that of the insulation layer [8]:

$$\begin{aligned} |k_4/k_{2e}|^2 &\ll 1 \\ |k_{2e}r_c|^2 &\ll 1 \end{aligned} \quad (1)$$

- The radius of the inner conductor a is such that [8]:

$$\begin{aligned} a &\ll h \\ k_{2e}a &\ll 1 \end{aligned} \quad (2)$$

Considering several values of the ratio r_c/a , a thin insulation is considered if it can be assumed that the following assumption holds: $1 \leq r_c/a \leq 2$. Moreover, a thick insulation is assumed if $r_c/a > 2$.

- The effective insulation layer is a non-lossy dielectric medium that is $\sigma_{2e} = 0$, so that $\tilde{\epsilon}_{r2e} = \epsilon_{2e}'^2$. Usually, Teflon is chosen ($\epsilon_{2e}' = 2$).
- The relative complex permittivity of the outer medium (index 4) writes as follows:

$$\tilde{\epsilon}_{r4} = \epsilon_4' - j \frac{\sigma_4}{\omega \epsilon_0} \quad (3)$$

- The complex wavenumbers in the several media are:

For the inner conductor (index L):

$$k_L = \beta_L + j\alpha_L \quad (4)$$

For the effective insulation layer (index $2e$):

$$k_{2e} = \beta_{2e} + j\alpha_{2e} = \omega \sqrt{\mu_0 \epsilon_0 \tilde{\epsilon}_{r2e}} \quad (5)$$

For the outer lossy dielectric medium:

$$k_4 = \beta_4 + j\alpha_4 = \omega \sqrt{\mu_0 \epsilon_0 \tilde{\epsilon}_{r4}} \quad (6)$$

- Then, we define the following complex index:

$$n_{2e4}^2 = \frac{k_{2e}^2}{k_4^2} \quad (7)$$

- The complex intrinsic impedances associated with the different media are:

$$\begin{cases} \tilde{\eta}_{2e} = \sqrt{\frac{\mu_0}{\epsilon_0 \tilde{\epsilon}_{r2e}}} \\ \tilde{\eta}_4 = \sqrt{\frac{\mu_0}{\epsilon_0 \tilde{\epsilon}_{r4}}} \end{cases} \quad (8)$$

- The current at the feed-point $z = 0$ is defined as follows:

$$I_0 = \frac{V_0}{Z_{in}} \quad (9)$$

(V_0 is assumed to be equal to 1V) where Z_{in} is the input impedance at the position of the feed-point $z = 0$, which will be defined later.

² a permittivity with a tilde notation indicates a complex variable

The reflection coefficient at the antenna feed-point is defined with respect to the reference impedance of 50 Ω , and for impedance matching consideration, the aim is to obtain an antenna with a low reflection coefficient S_{11dB} at the feed-point:

$$S_{11dB} = 20 \log_{10} \left(\frac{Z_{in} - 50}{Z_{in} + 50} \right). \quad (10)$$

3.2 Current Distribution

The analytical formulation based on the transmission line theory first introduced by R.W.P. King is now presented [8-10]. The insulated antenna (monopole or dipole) is treated as a lossy transmission line. In such a case, losses induced in the outer conductive medium are due to ohmic losses and radiation.

Considering at first a uniform antenna (made of a single section) aligned with the axis Oz , the current distribution versus z writes as follows:

$$I(z) = I_0 \frac{\sin(k_L(h - |z|))}{\sin(k_L h)} \quad (11)$$

where $I_0 = I(z = 0)$.

If the insulated antenna with the constant outer radius c is made of N multisections connected to each other along the axis Oz (each characterized by a proper inner conductor radius a^i and an insulation layer thickness $(r_c - a^i)$), we observe that distinct current distributions $I^i(z)$ are traveling inside each section i of the length h^i with the wavenumber k_L^i (see Fig. 1b). The current $I^i(z)$ associated with the section i is given by:

$$I^i(z) = I_0^i \frac{\sin(k_L^i(z_0^i + h^i - |z|) + j\theta_h^i)}{\sin(k_L^i h^i + j\theta_h^i)} \quad (12)$$

where z_0^i represents the lower end of the section i which the current enters, and z is the coordinate along the axis Oz ($z = 0$ corresponds to the feed-point). I_0^i is the current $I^i(z = z_0^i)$. θ_h^i is the phase angle that results from the loading effect of the sections connected upward to the section i .

It must be underlined that the current distribution follows the continuity relation at each position $z = z_0^i$: $I^i(z = z_0^i) = I^{i-1}(z = z_0^i)$.

The current in each of the N sections is determined using the several following steps:

1) At first, the characteristic impedances Z_c^i of each section have to be determined according to the following relation:

$$Z_c^i = \frac{\omega \mu_0 k_L^i}{2\pi k_{2e}^2} \left[\ln \left(\frac{r_c}{a^i} \right) + n_{2e4}^i F \right] \quad (13)$$

where $F = \frac{H_0^{(2)}(k_4 r_c)}{k_4 H_1^{(2)}(k_4 r_c)}$ is a constant parameter, and $H_0^{(2)}$ and $H_1^{(2)}$ are the Hankel functions of the second kind of order 0 and 1, respectively.

$$k_L^i = k_{2e} \frac{\sqrt{\ln(r_c / a^i) + F}}{\sqrt{\ln(r_c / a^i) + n_{2e4}^i F}} = \beta_L^i + j\alpha_L^i \quad (14)$$

Note that the ratio $|\alpha_L^i / \beta_L^i|$ represents a measure of the capacity of each section to transfer power to the surrounding medium by conduction, radiation, or the combination of both. Depending on the ratio $|\alpha_4 / \beta_4|$, and r_c / a^i , it must be remarked that $|\alpha_L^i / \beta_L^i|$ is larger for radiation when the losses for a given medium 4 are weaker. Moreover, from relation (14) it can be deduced that $|\alpha_L^i / \beta_L^i|$ can be made quite large when r_c / a^i is near one, and quite small when r_c / a^i is much greater than one. Thus, when r_c / a^i is large and $|\alpha_L^i / \beta_L^i|$ quite small, the transmission of power is made axially along the antenna like a low-loss transmission line, and when r_c / a^i is near one with $|\alpha_L^i / \beta_L^i|$ relatively large, the transmission is mainly made by conduction or radiation in the radial direction into medium 4 [9].

2) Starting at the top open-ended terminal of the antenna corresponding to the section $i = N$ at the position $z = h - h^N$ the phase $\theta_h^N = 0$ is assumed ($Z_{in} = \infty$). In a more general case, θ_h^i is expressed by:

$$\theta_h^i = \coth^{-1} \left(\frac{Z_{in}^{i+1}}{Z_c^i} \right) \quad (15)$$

Afterwards, the input impedance Z_{in}^i associated with this section can be calculated according to:

$$Z_{in}^i(z = z_0^i) = jC_{ant} Z_c^i \coth(k_L^i h^i + j\theta_h^i) \quad (16)$$

where $C_{ant} = 1$ in the case of a monopole, and $C_{ant} = 2$ in the case of a dipole.

Thus, the input impedances of the different sections are sequentially determined from the top end to the feed-point.

3.3 Electric Field Radiated

R. W. King has first proposed analytical expressions associated with the electric field radiated by a uniform insulated dipole in the lossy medium (index 4) surrounding the antenna. The solution of the Maxwell equations given in the cylindrical coordinates (ρ, φ, z) is expressed under its integral form. The electric field, formed of two components $E_{4r}(\rho, z)$ and $E_{4z}(\rho, z)$, includes both near-field and far-field variations. However, to solve the surface integrals over the insulation in both components, R. W. P. King has used an approximate numerical calculation, which leads to an inadequate solution in the vicinity of the insulation boundary. J. P. Casey has highlighted this inadequacy [11], and has thus proposed a numerical solution. Later, M. F. Iskander has formulated a solution which simplifies significantly the calculation of the electric field radiated, and allows to consider in particular a multisection antenna (monopole or dipole) for which no analytical solutions exist [12]. This simplified solution assumes that the current distribution along the axis Oz can be modeled by a linear array of elementary point sources localized at z' and distributed

along the antenna; they individually contribute to an infinitesimal electric field determined at a given position (ρ, z) and expressed in the local polar coordinates (r', θ') as (see Fig. 1a):

$$\begin{cases} E'_{4r}(r', \theta', z') = \frac{J'_e(z')}{2\pi} e^{-jk_z r'} \left(\frac{\eta_4}{(r')^2} + \frac{1}{j\omega \tilde{\epsilon}_4 (r')^3} \right) \cos \theta' \\ E'_{4\theta}(r', \theta', z') = \frac{J'_e(z')}{2\pi} e^{-jk_z r'} \left(\frac{j\omega \mu_0}{r'} + \frac{\eta_4}{(r')^2} + \frac{1}{j\omega \tilde{\epsilon}_4 (r')^3} \right) \sin \theta' \end{cases} \quad (17)$$

where $r' = \sqrt{\rho^2 + (z - z')^2}$, $\sin \theta' = \frac{\rho}{r'}$, and $\cos \theta' = \frac{(z - z')}{r'}$.

It must be underlined that in the case of a multisection antenna, a correction factor has to be applied to the current distribution $I^i(z')$, so as to represent more accurately the power dissipation in the near-field zone of the antenna as a function of the insulation thickness. This factor consists of an intensity modifying factor such as:

$$J'_e(z') = \frac{\beta'_L}{\alpha'_L} I^i(z'). \quad (18)$$

Otherwise, in the case of a uniform antenna, we have:

$$J'_e(z') = I^i(z'). \quad (19)$$

The projection of both elementary E-components in the plane (ρ, z) leads to:

$$\begin{cases} E'_{4\rho}(r', \theta', z') = E'_{4r}(r', \theta', z') \cos \theta' - E'_{4\theta}(r', \theta', z') \sin \theta' \\ E'_{4z}(r', \theta', z') = E'_{4r}(r', \theta', z') \sin \theta' + E'_{4\theta}(r', \theta', z') \cos \theta' \end{cases} \quad (20)$$

Then, the total electric field radiated by the insulated antenna in the surrounding medium (index 4) is expressed as follows:

$$\begin{cases} E_{4\rho}(r, \theta) = \int_{-h_1}^{h_2} (E'_{4r}(r', \theta', z') \cos \theta' - E'_{4\theta}(r', \theta', z') \sin \theta') dz' \\ E_{4z}(r, \theta) = \int_{-h_1}^{h_2} (E'_{4r}(r', \theta', z') \sin \theta' + E'_{4\theta}(r', \theta', z') \cos \theta') dz' \end{cases} \quad (21)$$

The parameters h_1 and h_2 have the following values: in the case of a monopole antenna $h_1 = 0$ and $h_2 = h$, and in the case of a dipole antenna $h_1 = h$ and $h_2 = h$.

4. Energy Absorbed in the Surrounding Medium

The electromagnetic field radiated in the lossy dielectric medium surrounding the insulated antenna with index 4 produces energy dissipation which is converted into heat. The energy per unit volume of the surrounding medium (tissue) dissipated in heat (W/m^3) is expressed as follows [11]:

$$\begin{aligned} P_{d4}(r, \theta) &= \frac{1}{2} \sigma_4 \vec{E}_4(r, \theta) \cdot \vec{E}_4^*(r, \theta) \\ &= \frac{1}{2} \sigma_4 (|E_{4\rho}(r, \theta)|^2 + |E_{4z}(r, \theta)|^2) \end{aligned} \quad (22)$$

The penetration depth δ of the electromagnetic field in the surrounding medium, which corresponds to the dis-

tance at which only 13.5 % of the maximum power absorbed remains, is equal to:

$$\delta = \frac{1}{\omega} \left[\frac{\mu_0 \epsilon_{r4} \epsilon_0}{2} \left(\sqrt{1 + \frac{\sigma_4}{\omega \epsilon_{r4} \epsilon_0}} - 1 \right) \right]^{-1/2}. \quad (23)$$

We assume that the power absorbed in a depth corresponding to 50 % of the maximum power is likely to produce a sufficient temperature rise. This depth is defined as:

$$d_{1/2} = \delta \frac{\ln(2)}{2}. \quad (24)$$

The distribution of the energy absorbed per unit of mass contained in a volume element of density ρ_c (kg/m^3) is called the Specific Absorption Rate (SAR). It is expressed by:

$$\text{SAR} = \frac{P_{4d}}{\rho_c}. \quad (25)$$

The SAR is related to the temperature rise ΔT ($^\circ\text{C}$) at the steady state through the equation:

$$\text{SAR} = k_c C \frac{\Delta T}{\Delta t} \quad (26)$$

where $k_c = 4186$ (J/kcal) and C is the specific heat of the medium (kcal/kg. $^\circ\text{C}$). It must be underlined that relation (26) does not take into account heat exchange with the blood flow.

5. Phased Antenna Array

Considering identical monopole or dipole antennas, with index $i = 1, \dots, L$ (see Fig. 2), positioned in an array in plane (x, y) , such that their driving point is localized at $z=0$ with coordinates $(x_{0i}, y_{0i}, 0)$, the components of the total electric field induced by the array at a given observation point (x, y, z) may be expressed as the sum of the complex elementary electric field associated with each antenna [15], [16]. In the case considered here, the first hypothesis is that the current distribution of a given antenna is not modified by the electromagnetic fields radiated by the others; so the distance between two antennas has to be greater than 2 or 3 penetration depth. The second hypothesis is that the antennas are parallel. The field components write as follows [16]:

$$\begin{cases} E_{4x}(x, y, z) = \sum_{i=1}^L \left(\frac{x - x_{0i}}{R_i} \right) E_{4\rho i} e^{j\varphi_i} \\ E_{4y}(x, y, z) = \sum_{i=1}^L \left(\frac{y - y_{0i}}{R_i} \right) E_{4\rho i} e^{j\varphi_i} \end{cases} \quad (27)$$

where $R_i = \sqrt{(x - x_{0i})^2 + (y - y_{0i})^2}$, $E_{4z}(x, y, z) = \sum_{i=1}^L E_{4z i} e^{j\varphi_i}$, and φ_i is the phase angle of the electric field of antenna i .

Therefore, the power absorbed per unit mass (SAR) in medium 4 is expressed by:

$$\text{SAR}(x, y, z) = \frac{1}{2} \frac{\sigma_4}{\rho_c} P_{4d_array}(x, y, z) \quad (28)$$

where the local power dissipated is:

$$P_{4d_array}(x, y, z) = |E_{4x}(x, y, z)|^2 + |E_{4y}(x, y, z)|^2 + |E_{4z}(x, y, z)|^2 \quad (29)$$

6. Results

Several antenna geometries have been considered to allow comparisons with results issued from the literature, considering different antenna structures, and also to illustrate the possibilities of the Matlab toolbox we have developed. In general, the simulation results allow to obtain plots of the current distribution along an antenna, a contour line chart of the power dissipated in a given plane inside the surrounding medium (a normalization has been defined in reference to a given power arbitrarily chosen by several authors from the antenna axis at $z = 1$ cm and $\rho = 2$ mm), and a 3D representation of the power dissipated in medium 4, for a fixed value of z (the normalization is adopted relative to the maximum power value).

At first, we considered uniform and multisection monopole antennas with the length $h = 6$ cm at the frequency $f = 500$ MHz as studied previously by Iskander et al. [12]. The insulation layer is supposed to be made of Teflon ($\epsilon'_{r2e} = 2$), and the surrounding medium is formed of muscle ($\epsilon'_{r4} = 52.5$, $\sigma_4 = 0.88$ S/m). The geometry characteristics are collected in Tab 1.

Uniform antenna	Multisection antenna (3 sections)
$h=60$ mm	$h=60$ mm
$r_c=1.7$ mm	$r_c=2.25$ mm
$a=0.794$ mm	$a_1=1.5$ mm ; $z=40$ to 60 mm
	$a_2=1.2$ mm ; $z=20$ to 40 mm
	$a_3=0.794$ mm ; $z=0$ to 20 mm

Tab. 1. Geometry parameters of monopole insulated antennas ($f=500$ MHz).

Considering the monopole antenna, the simulations lead to the following values associated with the wavenumber $k_L = 27.807 - 5.738j$ ($\beta_L h = 1.67 \approx \lambda_L$), the characteristic impedance $Z_c = 66.91 - 13.73j$, the input impedance $Z_{in} = -23.55 - 1.24j$, and the wavenumber of medium 4, $k_4 = 79 - 22j$ ($\lambda_4 = 7.95$ cm). The current distribution along the monopole is presented in Fig. 3. The isocurves of the dissipated power expressed in percentage relative to the reference power defined previously, are visualized on Fig. 4; they agree satisfactorily with the results issued from [9]. We observe that the power dissipated along that antenna does not appear uniform and decreases rapidly with the distance to the antenna. The higher dissipated power appears located close to the feed-point. It must be underlined that the 13 percent line corresponds to $1/e^2$ values of the power dissipated, which is usually defined as the power depth of penetration. To obtain a sufficient heating around the antenna, it appears that the heating region is far smaller than the region delimited by the 50 percent line.

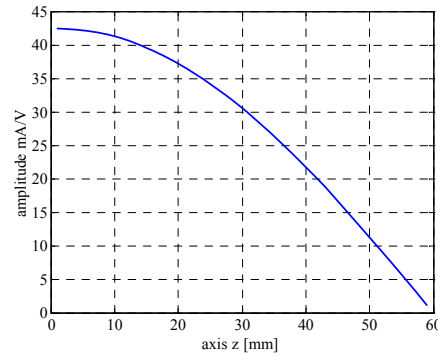


Fig. 3. Current distribution $I(z)$ along the antenna in the case of a uniform insulated monopole antenna ($f=500$ MHz).

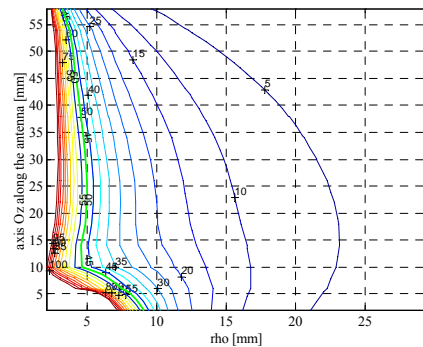


Fig. 4. Contour line chart of the normalized power dissipated versus the radial distance r from the antenna (reference $z=10$ mm, $r=2$ mm) in the case of a uniform insulated monopole antenna ($f=500$ MHz).

In the case of a multisection antenna working at the same frequency, the thicker dielectric layer has to be placed at the feed-point where the power dissipation is maximum, in order to reduce losses close to the insulation surface. Thus, several sections characterized by their proper dielectric thickness are positioned along the antenna to improve the uniformity of the heating pattern. Fig. 5 shows the corrected current distribution $J_e(z)$ according to [12]. Starting from section 1 to section 3, the parameters r_c/a^i and $|\alpha_L^i/\beta_L|$ have the following values: 1.5 and 0.248 for section 1, 1.875 and 0.228 for section 2, and 2.83 and 0.198 for section 3. In Fig. 6 the heating pattern highlights the fact that the power dissipated is more uniform compared to the previous case of a uniform antenna; this pattern is similar to the one obtained in [12]. The parameters associated with the different sections have to be optimized in order to obtain an efficient coupling between the antenna and the dissipative medium.

We consider now an array of 4 parallel symmetric dipoles positioned at the corners of a 20 mm square (size range of a tumor) with their feed-points at $z = 0$. The dipoles are working at the frequency $f = 915$ MHz with the characteristics defined by King in [8-11], such as $h = 30$ mm, $r_c = 0.8$ mm, $a = 0.47$ mm, $\epsilon'_{r2e} = 1.373$, $\epsilon'_{r4} = 42.5$, and $\sigma_4 = 0.88$ S/m. The current distribution along each antenna is plotted on Fig. 7. The electric field of a given antenna is obtained as follows: at first, the antenna is located at the origin and the electric field is determined

in the plane $(\rho\theta z)$ from relation (21). Then, by a rotation around the axis Oz , we can determine the field in the additional plane (xOy) . Afterwards, the field map is shifted to move the initial antenna from the origin to the actual position of the given antenna in the plane (xOy) . A linear interpolation has been used to transform the geometrical representation from the cylindrical coordinates to the cartesian coordinates, best suited to the positioning of the antennas. The simulation results of the power dissipated in the surrounding medium and presented in Fig. 8 and Fig. 9 highlight the effect of the variation of relative phases between each antenna ($\Delta z = h/30$, $\Delta x = \Delta y = 0.5$ mm); these simulations have been compared to studies performed previously by several authors [14-16]. Defining a cut plane (xOy) corresponding to $z_0 = 10$ mm, we remark that according to Fig. 7, in the presence of identical phases, the maximum power is positioned at the center of the array; in such case, this point is equidistant from all antennas, and the complex electric fields add coherently. This maximum location can be shifted by using phase differences between the antennas.

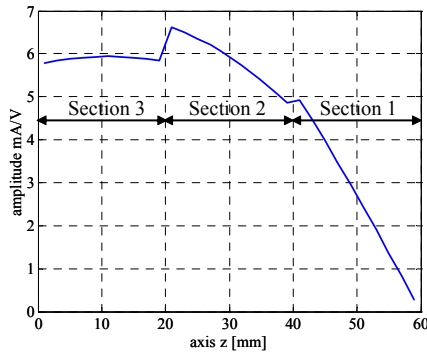


Fig. 5. Current distribution $J_z(z)$ along the antenna in the case of a multisection (3 sections) monopole antenna ($f=500$ MHz).

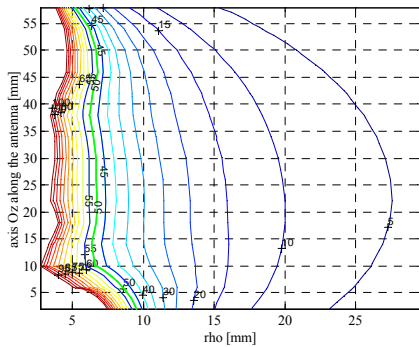


Fig. 6. Contour line chart of the normalized power dissipated versus the radial distance r from the antenna (reference $z=10$ mm, $r=2$ mm) in the case of a multisection (3 sections) monopole antenna ($f=500$ MHz).

As an illustration, Fig. 8 and Fig. 9 show two different results where two phases equal to 0° and 180° , and 0° and 90° respectively, have been considered for pairs of antennas. We remark that in the case of a 180° phase delay, hot spots of the same amplitude remain at the location of the antennas; between antennas with different phases, the power dissipated decreases rapidly. A weak dissipated power is observed between antennas of identical phase. In

the case of a 90° phase delay, the hot spots associated with the position of the antennas are not identical, and an important and quasi uniform power deposition is noticed between both antennas of the same phase with the lowest value 0° (see Fig. 10).

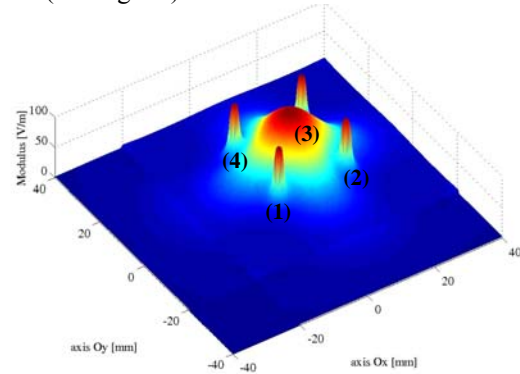


Fig. 7. Power dissipated in medium 4 ($\phi_1=\phi_2=\phi_3=\phi_4=0^\circ$; $z_0=1$ cm) in the plane (xOy) considering an array of uniform and symmetric dipoles ($f=915$ MHz, $z_0=1$ cm).

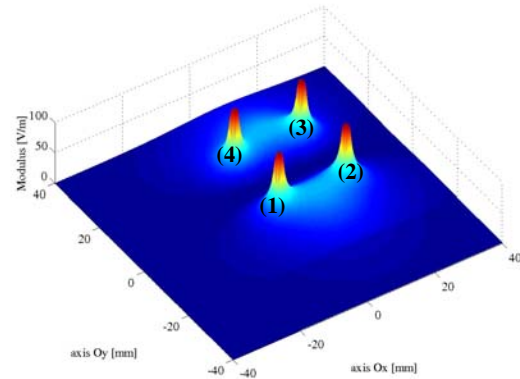


Fig. 8. Power dissipated in medium 4 ($\phi_1=\phi_2=0^\circ$; $\phi_3=\phi_4=180^\circ$; $z_0=1$ cm) considering an array of uniform and symmetric dipoles ($f=915$ MHz, $z_0=1$ cm).

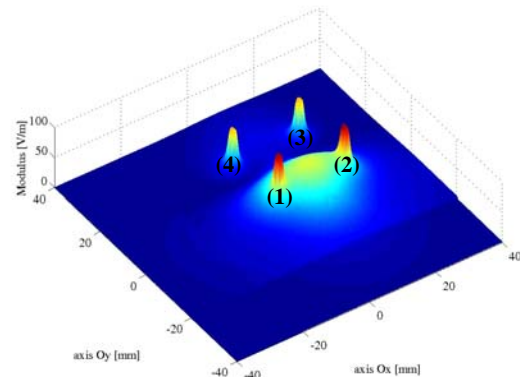


Fig. 9. Power dissipated in medium 4 ($\phi_1=\phi_2=0^\circ$; $\phi_3=\phi_4=90^\circ$; $z_0=1$ cm) considering an array of uniform and symmetric dipoles ($f=915$ MHz, $z_0=1$ cm).

7. Conclusion

In this paper, we have reviewed the principles of microwave interstitial antennas for hyperthermia applications by presenting the several electromagnetic modeling developed since the 1970's. The main analytical electromag-

netic models have been implemented in Matlab interface, and are freely available at request. These modeling consider different antenna geometries (uniform or multisection) and allow also to position antennas in a parallel array. Considering initial conditions previously specified by several authors, we have presented a few simulation results associated with several antenna geometries (uniform or multisection) studied separately at first, and afterwards considered in an array. The different 2D and 3D plots agree satisfactorily with the results issued from the literature. Since the 1990's, electromagnetic and thermal numerical modeling have emerged to simulate more real geometries of antennas and biological tissues [17-19]. These models rely mainly on the FDTD and the FEM methods.

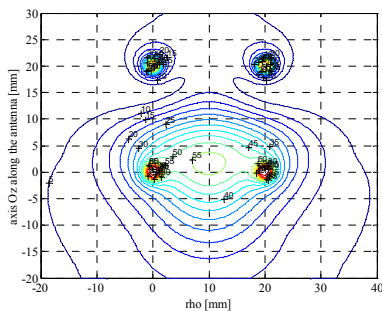


Fig. 10. Contour line chart in percentage of the maximum power dissipated in medium 4 ($\phi_1=\phi_2=0^\circ$; $\phi_3=\phi_4=90^\circ$; $z_0=1$ cm) considering an array of uniform and symmetric dipoles ($f=915$ MHz, $z_0=1$ cm).

Acknowledgements

The author would like to thank Emile Hiltbrand from CERMA, Archamps (France) as a physician for sharing his experience in hyperthermia applications.

References

- [1] CONWAY, J., ANDERSON A. P. Electromagnetic techniques in hyperthermia. *Clin. Phys. Physiol. Meas.*, 1986, vol. 7, no. 4, p. 287 – 318.
- [2] CHOU, C. K. Application of electromagnetic energy in cancer treatment. *IEEE Trans. Instrum. Meas.*, 1988, vol. 37, no. 4, p. 547 – 551.
- [3] SIMON, C. J., DUPUY, D. E., MAYO-SMITH, W. W. Microwave ablation: Principles and applications. *Radiographics*, vol. 25, 2005, p. 69-83.
- [4] Mini-Special Issue on RF/Microwave applications in medicine, Part 1, 2. *IEEE Trans. Microw. Theory Tech.*, 2000, vol. 48, no. 11, p. 1783 – 2198.
- [5] STAUFFER, P. R. Evolving technology for thermal therapy of cancer. *Int. J. Hyperthermia*, vol. 21, no. 8, 2005, p. 731 – 744.
- [6] HAEMMERICH, D., LASEKE, P. F. Thermal tumour ablation: Devices, clinical applications and future directions. *Int. J. Hyperthermia*, vol. 21, no. 8, 2005, p. 755 – 760.
- [7] JOINES, W. T., ZHANG, Y., LI, C., JIRTLE, R. L. The measured electrical properties of normal and malignant human tissues from 50 to 900 MHz. *Medical Physics*, vol. 21, no. 4, 1994, p. 547 – 550.
- [8] KING, R. W. P., LEE, K. M., MISHRA, S. R., SMITH, G. S. Insulated antenna: Theory and experiment. *J. Appl. Phys.*, vol. 45, no. 4, 1974, p. 1688 – 1697.
- [9] KING, R. W. P., SHEN, L. C., WU, T. T. Embedded insulated antennas for communication and heating. *Electromagnetics*, 1981, vol. 1, p. 51 – 72.
- [10] KING, R. W. P., TREMBLY, B. S., STROHBEHN, J. W. The electromagnetic field of an insulated antenna in a conductive or dielectric medium. *IEEE Trans. Microw. Theory Tech.*, vol. 31, no. 7, 1983, p. 574 – 583.
- [11] CASEY, J. P., BANSAL, R. The near field of an insulated dipole in a dissipative dielectric medium. *IEEE Trans. Microw. Theory Tech.*, 1986, vol. 34, no. 4, p. 459 – 463.
- [12] ISKANDER, M. F., TUMEH, A. M. Design optimization of interstitial antennas. *IEEE Trans. Biomed. Eng.*, vol. 36, no. 2, 1989, p. 238.
- [13] CLIBBON, K. L., MCCOWEN, A. Efficient computation of SAR distributions from interstitial microwave antenna arrays. *IEEE Trans. Microw. Theory Tech.*, 1994, vol. 42, no. 4, p. 595 – 601.
- [14] WU, L. K., SU, D. W. F., TSENG, B. C. A fast algorithm for computing field radiated by an insulated dipole antenna in dissipative medium. *IEEE Trans. Microw. Theory Tech.*, vol. 44, no. 12, 1996, p. 2290 – 2293.
- [15] STUART TREMBLY, B., WILSON, A. H., SULLIVAN, M. J., STEIN, A. D., WONG, T. Z., STROHBEHN, J. W. Control of the SAR pattern within an interstitial microwave array through variation of antenna driving phase. *IEEE Trans. Microw. Theory Tech.*, vol. 34, no. 5, 1986, p. 568 – 571.
- [16] ZHANG, Y., JOINES, W. T., OLESON, J. R. Microwave hyperthermia induced by a phased interstitial antenna array. *IEEE Trans. Microw. Theory Tech.*, vol. 38, no. 2, 1990, p. 217 – 221.
- [17] CHERRY, P. C., ISKANDER, M. F. FDTD analysis of power deposition patterns of an array of interstitial antennas for use in microwave hyperthermia. *IEEE Trans. Microw. Theory Tech.*, vol. 40, no. 8, 1992, p. 1692 – 1700.
- [18] CHERRY, P. C., ISKANDER, M. F. Calculations of heating patterns of an array of microwave interstitial antennas. *IEEE Trans. Biomed. Eng.*, vol. 40, no. 8, 1993, p. 771 – 778.
- [19] EPPERT, V., TREMBLY, B. S., RICHTER, H. J. Air cooling for an interstitial microwave hyperthermia antenna: Theory and experiment. *IEEE Trans. Biomed. Eng.*, vol. 38, no. 5, 1991, p. 450 – 460.

About the Author ...

Florence SAGNARD (*1965 Paris, France) received the engineer diploma and the D.E.A. degree in electronics from the Univ. Pierre and Marie Curie, France, in 1990, and the Ph.D. degree from the Univ. of Orsay, France, in 1996. From 1990 to 1993, she was an Engineer working on military electronic systems. From 1993 to 1996, she was with CEA at Bruyères-Le-Châtel and ONERA at Chatillon to work on the characterization of heterogeneous dielectric absorbing materials for radar applications. In 1997, she became an Assistant Professor at the Univ. of Marne-La-Vallée, France. Her research interests were focused on the microwave characterization of building materials by free-space techniques. From 2002 to 2007, she was on secondment and joined as a full-time researcher the Inst. of Electronics and Telecommunications of Rennes (IETR—UMR CNRS 6164) in the National Inst. of Appl. Sciences of Rennes (INSA), to devote her work on ultra-wide band wave-matter interactions for indoor communications. In 2005, she obtained her Habilitation à Diriger des Recherches (HDR) from the Univ. of Marne-La-Vallée. Since 2007, she has been working as a full-time researcher at the regional civil engineering laboratory of Rouen (France) on GPR radars.